ERF2011-135

GEOMETRIC OPTIMISATION OF A GURNEY FLAP HINGE-LESS DEPLOYMENT SYSTEM FOR A HELICOPTER MODEL BLADE

A. Paternoster, R. Loendersloot, A. de Boer, R. Akkerman

Structural Dynamics and Acoustics,
Faculty of Engineering Technology,
University of Twente,
Enschede, Netherlands
Email: a.r.a.paternoster@utwente.nl

ABSTRACT

Following a comparative study on shape morphing and adaptive systems to improve rotorcraft efficiency, the Green Rotorcraft consortium has selected the Gurney flap technology as demonstrator of a smart adaptive rotorblade within the Clean Sky Joint Technology Initiative [1]. The aim of such a system is to actively increase helicopter overall performance by improving lift and alleviating static and dynamic stall on the retreating side of the helicopter [2, 3]. The Gurney flap technology will be subjected to various tests, prior to manufacturing a full-scale demonstrator. Along with wind tunnel and whirl tower tests on full blade sections, a reduced-scale blade is required to be tested on a rotary support in a wind tunnel. The aim is to have a fully operational mechanism in a 1/8th-scale blade. A specific system needs to be designed for this smaller model blade. The specifications for the model blade mechanism are more challenging compared to the full model blade. The blade tip speed must remain the same between the two blades. Therefore, the model blade rotation speed and centrifugal loads greatly increase. Piezoelectric patch actuators combined with flexible beams are chosen to design a fast and robust mechanism, which would fit inside the model blade and support the large centrifugal loads. A mechanism is modeled using Finite Element Analysis tools and its geometry is optimised using a surrogate optimisation to maximise displacement and force. The optimised geometry has a Z-shape profile and maximise displacement and force. The force generated is sufficient to counter directly the force of the airflow on the flap. However, the displacement and the mechanical work are not large enough to deploy directly the Gurney flap as a conventional flap. The deployment time remains insufficient as well. Building on these results, refined geometries are under investigation using the same optimisation process.

INTRODUCTION

Shape morphing and adaptive systems appear to be promising technologies for improving rotorcraft performances and efficiency [3–6]. The Green Rotorcraft Consortium have reviewed active concepts in the scope of the European Clean Sky Joint Technology Initiative to improve helicopter transportation on the following aspects: fuel consumption and performances, active vibration control and active noise control [7]. The Gurney flap technology was selected as a demonstrator of a smart adaptive rotorblade [1]. The Gurney flap consists in a small flap, which length measures typically 2% of the chord length, placed at of the rotorblade's trailing edge as shown in Figure 1. It improves the lift of the blade at a small drag penalty. Overall, the lift over drag coefficient increases over a large range of angles of attacks [2, 3, 8]. Moreover, the Gurney flap alleviates the static and dynamic stall of the blade [9].
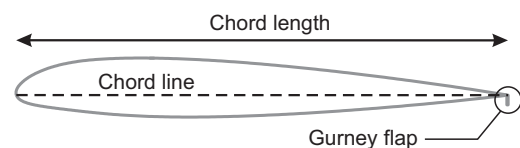
Figure 1: Sketch of a profile with a 2% long gurney flap at the trailing edge.

Control strategies

Depending on the actuation profile as the blade goes around the helicopter, the Gurney flap can provide a number of enhancements. The flap can be deployed to provide a significant lift increase in specific situations during the rotorcraft mission like take-off, landing and hovering. The blade providing more lift, the speed rotation of the turbine can be decrease which reduces the helicopter noise. Secondly, the Gurney flap

can be combined with sensors to measure and actively damped the blade vibrations. This would improve the transportation quality as well as reduce the noise induced by vibrations. Finally, the Gurney flap can be used as a mean to redistribute lift between the advancing blade and the retreating blade. When a helicopter goes forward, a lift unbalanced is created by the mismatch of airflow speed between two opposite blades as shown in Figure 2. At high speeds the retreating blade experience stall and counter flow close to the blade's root. This effect limits the maximum speed of a helicopter. Deploying the Gurney flap on the retreating side of the helicopter increases the lift for the retreating blade and improves the stall behaviour [1]. This third control strategy was selected for more investigation by the IGOR Consortium for the actuation of the Gurney flap.
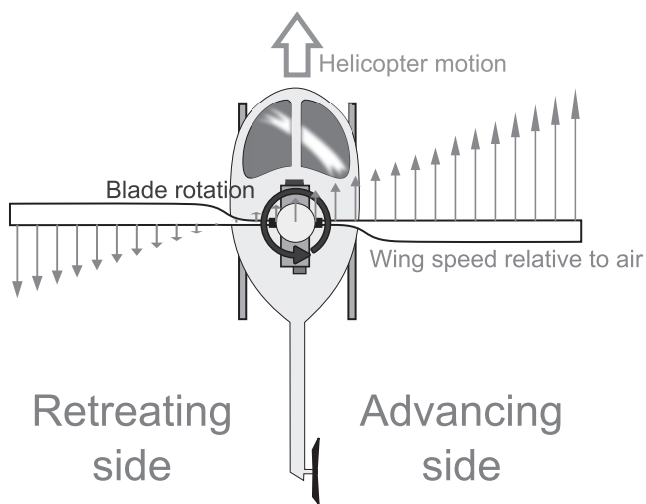
Figure 2: Airspeed imbalance between the two sides of a helicopter in motion.

Demonstrating the selected technology

Demonstrating the relevance of the chosen technologies requires mechanical and aerodynamic testing. A full-size blade with the final deployment system will be tested in a wind tunnel to verify the mechanism behaviour under static loading and the aerodynamic improvements provided by the Gurney flap. A whirl tower test is also required to have a better understanding of the coupling between the dynamics of the mechanism and the centrifugal loads. Finally a model blade will be mounted on a rotary support in a wind tunnel to assess the performance improvement provided by the Gurney flap for specific flight conditions and be a test ground for active control algorithms. The aim is to design and manufacture a model blade which includes a fully operational Gurney flap mechanism. The model blade length should be one eighth of the full-scale blade length as defined in the project definition

[10]. The profile chosen in this study is the Naca 23012 profile, which provided a common base for all partners at the start of the project. However, the full-scale system cannot be easily scale-down. A new mechanism need to be designed for the model blade to meet requirements specific to the model blade and the planned wind-tunnel test.

This article presents the work done on choosing and optimizing an actuation design for deploying a Gurney flap according to constraints encountered in a model blade.

METHODS

Constraints evaluation

Before designing the mechanism, the constraints affecting the helicopter blade are studied. The specifications of the full blade are shown in Table 1. Having a faithful model blade requires the tip speed of the model blade to be equal to the tip speed of the full blade. Therefore reducing the scale implies to increase the rotation speed and quadratically increase the centrifugal loads along the blade.

Table 1: Specifications of the Naca 23012 profile according to the baseline blade definition [10].

Chord length	650	mm
Blade length	8.14	m
Rotation speed	26.26	rad/s
Tip speed	214	m/s

The Gurney flap efficiency is linked to the deployment profile on the helicopter retreating side. It has been evaluated that deploying the Gurney flap within 10 degrees of sweeping angle led to optimal results in performance [1]. Again, as the rotation speed is larger with the model blade, the time requirement for the model blade mechanism is much smaller.

The force necessary for the mechanism's actuation is derived from simulations with a fixed Gurney flap. The worst-case is considered by taking the blade tip's speed as the flow speed. A quasi-static CFD simulation calculates the moment the flow induces on the Gurney flap for various angles of attacks as shown in Figure 3. At 12 degrees of attack, the flow induces a moment of 33 mN.m per meter of wingspan on the Gurney flap root. The block force and the mechanical work required by the mechanism are derived from this figure. The spec-

ifications of the mechanism are summarised in Table 2 per meter of wingspan for an eighth-scale model blade.

Table 2: Specifications of the model blade and the deployment mechanism.

Chord length	80	mm
Blade length	1	m
Tip speed	214	m/s
Peak g-acceleration	4700	g
Holding force	60	N/m
Mechanical work	55	mJ/m
Deployment time	0.83	ms
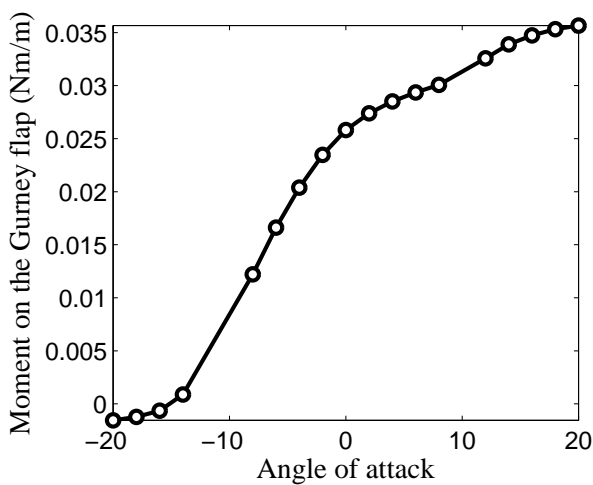
Figure 3: Moment per meter of wingspan acting on the root of a 2% Gurney flap placed at the trailing edge for various angles of attack.

Piezoelectric actuators

Piezoelectric material converts electrical power into mechanical power [11]. They are able to operate at great speeds in very demanding environments [12]. Moreover they can undergo a large number of cycles before having their performances reduced. Various actuation technologies were considered and selected according to their performances and their response time [13]. Piezoelectric actuators came ahead for the model blade mechanism due the short deployment time required. The disadvantage of using piezoelectric actuator is their small deformation output. Thus, piezoelectric actuators require amplification mechanisms to convert high force and small displacement into meaningful motion.

Actuation mechanism

Among piezoelectric actuators, Macro Fibre Composite piezoelectric actuator (MFC) from Smart-Material were selected for their good performances and form factor. MFCs as shown in Figure 4 are piezoelectric patch actuators. They are small and can be custom made. Table 3 details the performances of one MFC reference from Smart-Material.

Table 3: Specifications of MFC 4010-P1 by Smart-Material [14].

Active length	40	mm
Active width	10	m
Free displacement	56	μm
Block force	126	N
Maximum voltage	1500	V
Fatigue limit	10^9	cycles

To amplify the small displacements, MFCs are bonded onto flexible beams. When a voltage is applied on the piezoelectric actuator, strains generated in the piezoelectric actuator are transferred to the beam which bends depending on the voltage applied. The tip displacement of the beam is multiple times larger than the piezoelectric free displacement. The beam length is used to tune the displacement amplification. A mechanism made of flexible beams with piezoelectric actuators is investigated to provide sufficient displacement at the trailing edge of the model rotor blade while alleviating the centrifugal force. The connection between the beams are made with flexible hinges to avoid sensitivity to centrifugal loads and vibrations.
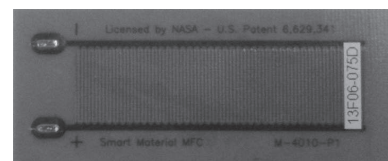
Figure 4: Picture of 4010-P1 Macro Fibre Composite manufactured by Smart Material.

Geometrical optimisation

First a basic structure is modelled using a finite element package that contains piezoelectric elements. The aim is to provide as much horizontal displacement as possible close to the trailing edge, where the Gurney flap need to be deployed. That structure consists in an upper beam linked to the D-spar of the helicopter blade. This upper part is connected to a middle arm that is itself linked to the lower arm which transmit horizontal

motion to the trailing edge. Both upper and lower arms follow the curvature of the blade profile to use as much space as possible. The piezoelectric actuator is bonded onto the upper arm. The model is a 2D-model that uses plain strain approximation. MFC piezoelectric properties are simplified to work in this 2D model. The quasi-static displacement at the end of the lower arm is retrieved from the simulation when 1200 V are applied on the piezoelectric element. No other constraint being applied on the mechanism, this displacement is the free displacement of the actuation mechanism. This model is then parametrized with geometrical variables, which are investigated by the optimisation: the lengths of the upper and lower arm and the curvature of the middle arm as shown in Figure 5.

a: length of the upper arm
b: length of the lower arm
c: curvature of the middle arm
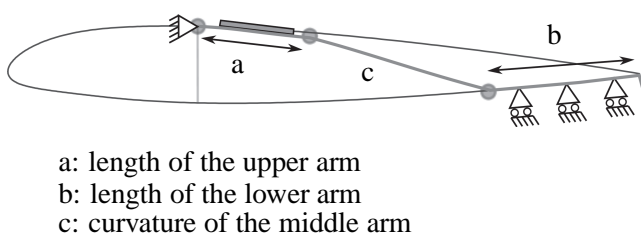
Figure 5: Geometrical parameters used for the optimisation of the finite element analysis.

A surrogate optimisation is chosen because it can solve multi-variables problems and requires a limited number of iterations [15, 16]. For that reason, this optimisation procedure is often used with Finite Element Analysis (FEA) to reduce the cost in computation time. It consists in two stages as shown in Figure 6. The first stage investigates the design space by testing a distribution of combination of variables. From these results, a surrogate function is evaluated. In this case the function gives an approximation of the displacement of the actuation mechanism for every combination of arms lengths and curvature. The second stage is the optimisation loop itself. The function maximum is found using a gradient-based algorithm. The FEA is run again for the combination of variables at the maximum. Then the surrogate function and its maximum are evaluated again until the termination criteria is met: less that 0.01% improvement between two successive loops.

RESULTS

After 30 initial combinations of variables, the surrogate function is calculated. The termination criteria is met within 10 iterations as shown in Figure 8. The optimised structure displays a Z-shape profile displayed in
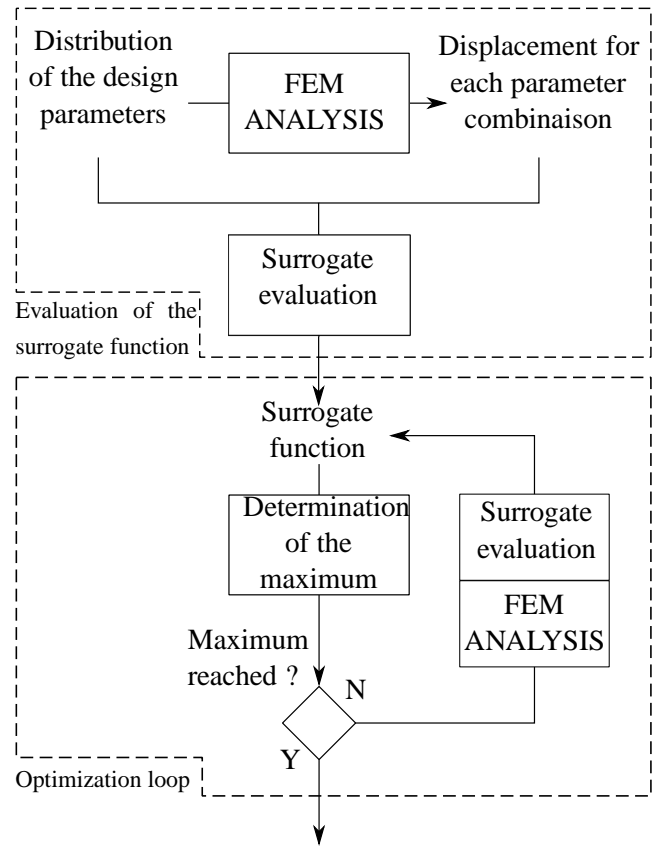
Figure 6: Flowchart detailing the evaluation of the surrogate function and the optimization loop.

Figure 7. The free displacement achieved by the optimised actuation mechanism is 0.81 mm. This displacement is insufficient to directly slide out the Gurney flap length (1.6 mm) but might be enough for deploying the Gurney flap by rotation. The block force is obtained by clamping the lower arm length and extracting the force from a new simulation. The resulting block force is 200 N, which is sufficient to directly sustain the force caused by the airflow. Assuming the actuation system behaviour is linear between the free displacement and the block force case, the characteristic curve is derived from these two figures. Intersection between the characteristic curve and the mechanism stiffness gives the working point as shown in Figure 9. An estimation of the mechanical work is given by the force and displacement found at this point. The mechanical work derived (33 mJ/m) is not sufficient to meet the 55 mJ/m required.
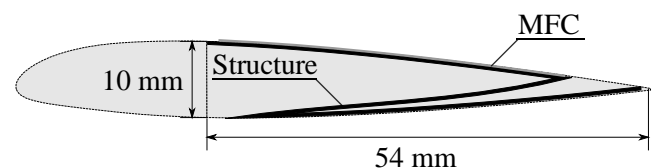
Figure 7: Resulting actuation mechanism and its dimensions after the geometrical optimisation.
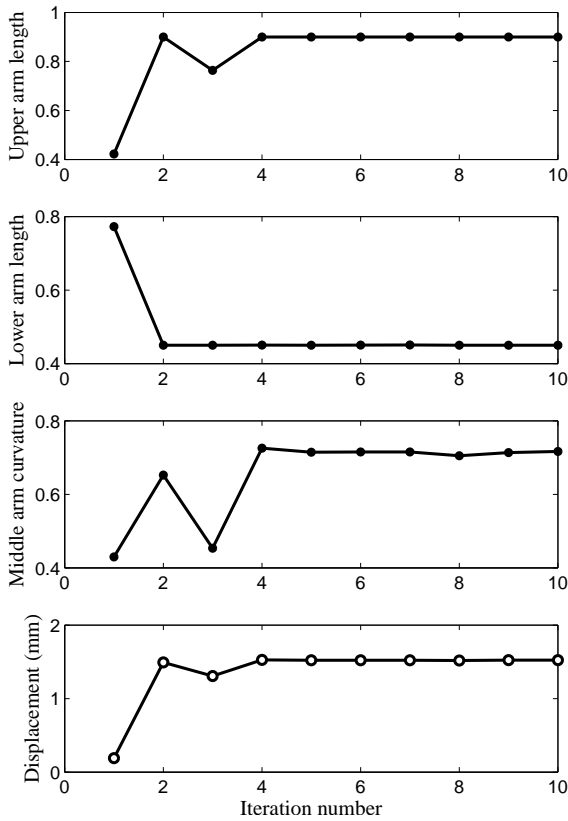
Figure 8: Convergence of the three design parameters and the displacement obtained with the FEA. The dimensions of the arms and the curvature are set in chord length percentage.
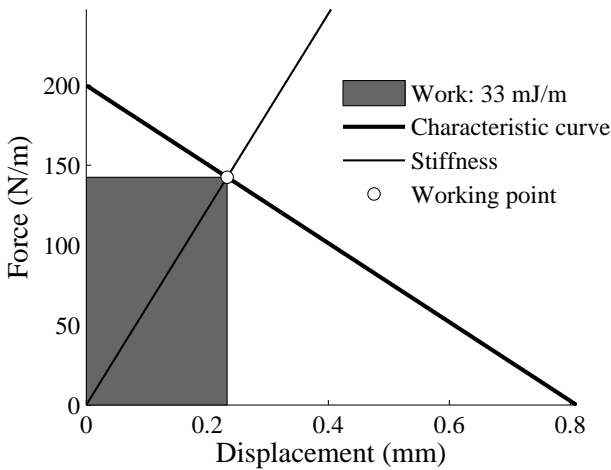
Figure 9: Characteristic curve of the actuation mechanism and graphical determination of the mechanical work.

In this first optimisation, the objective set was the displacement. Changing the objective to a parameter that takes into account both force and displacement leads to the very same mechanism.

A transient analysis is performed to obtain the response time when a step voltage is applied. The displacement according to time is shown in Figure 10. The quasi-static displacement is achieved at 1.3 ms. The deployment time depends on the amount of piezoelec-

tric material to induce motion. The optimisation maximises the upper arm length and therefore the length of the piezoelectric component and the deployment speed. New geometrical parameters such as the thickness of the bending beams need to be considered to bring the deployment time closer to the requirements.
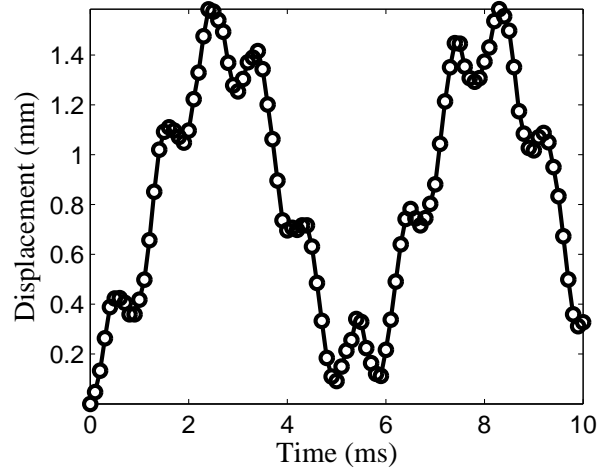
Figure 10: Displacement of the arm according to time when applying a step voltage to the piezoelectric actuator.

CONCLUSION AND FUTURE WORK

The surrogate optimisation scheme applied to the optimisation of the geometry of an actuation mechanism led to a novel Z-shape profile that maximised both force and displacement. The resulting structure delivers enough block force to maintain the Gurney flap deployed in the airflow. However, the work and the deployment speed remain insufficient for the specifications set.

Future work will refine the geometry presented in this article by including more geometrical variables using the same optimisation procedure. Deployment time will be set as an objective of the optimisation. Finally, less demanding deployment methods will be considered to slide the Gurney flap out instead of a conventional deployment by rotation.

Designing an actuation mechanism relies on both the actuation technology and the link which transmits displacement and force. The surrogate optimisation described here is suitable for such an investigation. It contributes to develop both the model and the full-scale blades with active parts. Finally, the robustness of piezoelectric flexible actuation system makes them a good candidate for performing in tough environments while keeping down the complexity and the number of parts.

ACKNOWLEDGEMENT

REFERENCES

[1] W. et al Maybury. GRC1.1 Technology Review Document. Technical report, CS JU/ITD GRC/RP/1.1/31005, 2010.

[2] M.D. Maughmer and Götz Bramesfeld. Experimental Investigation of Gurney Flaps. *Journal of Aircraft*, 45(6):2062–2067, November 2008.

[3] J. Wang, Y. Li, and K. Choi. Gurney flap-Lift enhancement, mechanisms and applications. *Progress in Aerospace Sciences*, 44(1):22–47, January 2008.

[4] R.M. Barrett. Design, development, and testing of a solid state adaptive rotor. *Proceedings of SPIE*, 422:424–435, 1998.

[5] C. E.S. Cesnik, W. K. Wilkie, and M. L. Wilbur. Design and Manufacturing of a Model-scale Active Twist Rotor Prototype Blade. *Journal of Intelligent Material Systems and Structures*, 19(12):1443–1456, May 2008.

[6] M. Thiel. *Actuation of an active Gurney flap for rotorcraft applications*. PhD thesis, The Pennsylvania State University, 2006.

[7] CleanSky - Green Rotorcraft project webpage. http://www.cleansky.eu/content/page/grc-green-rotorcraft. On the WWW, May 2010.

[8] M. Thiel and G.A. Lesieutre. New Actuation Methods for Miniature Trailing-Edge Effectors for Rotorcraft. In *AIAA/ASME/ASCE/AHS/ASC Structures, Structural Dynamics, and Materials Conference*, number May, 2009.

[9] K. Yee, W.N Joo, and D.H. Lee. Aerodynamic Performance Analysis of a Gurney Flap for Rotorcraft Application. *Journal of Aircraft*, 44(3):1003–1014, May 2007.

[10] W. Maybury, A. D'Andrea, R. Hilditch, P. Beaumier, and C. Garcia-Duffy. Baseline Blade Definition for GRC1.1. Technical report, CS JU/ITD GRC/RP/1.1/31002, 2009.

[11] I. Chopra. Review of State of Art of Smart Structures and Integrated Systems. *AIAA Journal*, 40(11):2145–2187, November 2002.

[12] R.B. Williams, Gyuhae Park, D.J. Inman, and W.K. Wilkie. An overview of composite actuators with piezoceramic fibers. *Proceeding of IMAC XX*, pages 4–7, 2002.

[13] A. Paternoster, A. DeBoer, R. Loendersloot, and R. Akkerman. Actuators for Smart Applications. In *Proceedings of the ASME 2010 Conference on Smart Materials, Adaptive Structures and Intelligent Systems*. Asme, 2010.

[14] Smart material website. http://www.smart-material.com/. On the WWW, May 2011.

[15] D. Akcay Perdahcioglu. *Optimizing the dynamic behavior of structures using substructuring and surrogate modeling*. PhD thesis, Enschede, July 2010.

[16] A.I.J. Forrester, A. Sóbester, and A.J. Keane. *Engineering design via surrogate modelling: a practical guide*. John Wiley & Sons Ltd., 2008.